HHS Public Access

Author manuscript

J Mol Biol. Author manuscript; available in PMC 2015 October 23.

Published in final edited form as:

J Mol Biol. 2008 June 27; 380(1): 51–66. doi:10.1016/j.jmb.2008.03.076.

Engineered bacterial outer membrane vesicles with enhanced functionality

Jae-Young Kim[1,†], **Anne M. Doody**[1,2,†], **David J. Chen**[1], **Gina H. Cremona**[1], **David Putnam**[1,2], and **Matthew P. DeLisa**[1,2]

[1]School of Chemical and Biomolecular Engineering, Cornell University, Ithaca NY 14853 USA

[2]Department of Biomedical Engineering, Cornell University, Ithaca NY 14853 USA

Abstract

We have engineered bacterial outer membrane vesicles (OMVs) with dramatically enhanced functionality by fusing several heterologous proteins to the vesicle-associated toxin ClyA of *Escherichia coli*. Similar to native unfused ClyA, chimeric ClyA fusion proteins were found localized in bacterial OMVs and retained activity of the fusion partners, demonstrating for the first time that ClyA can be used to co-localize fully functional heterologous proteins directly in bacterial OMVs. For instance, fusions of ClyA to the enzymes β-lactamase and organophosphorus hydrolase resulted in synthetic OMVs that were capable of hydrolyzing β-lactam antibiotics and paraoxon, respectively. Similarly, expression of an anti-digoxin single-chain Fv antibody fragment fused to the C-terminus of ClyA resulted in designer “immuno-MVs” that could bind tightly and specifically to the antibody’s cognate antigen. Finally, OMVs displaying green fluorescent protein fused to the C-terminus of ClyA were highly fluorescent and, as a result of this new functionality, could be easily tracked during vesicle interaction with human epithelial cells. We expect that the relative plasticity exhibited by ClyA as a fusion partner should prove useful for: (i) further mechanistic studies to identify the vesiculation machinery that regulates OMV secretion and to map the intracellular routing of ClyA-containing OMVs during invasion of host cells; and (ii) biotechnology applications such as surface display of proteins and delivery of biologics.

Introduction

Protein translocation is a highly conserved process that is essential to all life. Extracellular secretion of virulence factors is a strategy utilized by invading bacteria to establish a colonization niche, communicate with host cells, and modulate host defense and response. With few exceptions, bacterial protein secretion systems are characterized by the membrane translocation of a single protein or else small protein complexes.[1; 2; 3; 4; 5] Recently, however, the production and release of outer membrane vesicles (OMVs) has been

Address correspondence to: Matthew P. DeLisa, 254 Olin Hall, Cornell University, Ithaca, NY 14853 USA; phone: 607-254-8560; fax: 607-255-9166; md255@cornell.edu.

[†]These authors contributed equally to the studies presented in this manuscript

demonstrated as a novel secretion mechanism for the transmission of a diverse group of proteins and lipids to mammalian cells.[6] OMVs are small proteoliposomes with an average diameter of 50–200 nm that are constitutively released from the outer membrane of pathogenic and non-pathogenic species of Gram-negative bacteria during growth.[7] Biochemical analysis has demonstrated that OMVs are comprised of outer membrane proteins, lipopolysaccharide, phospholipids and soluble periplasmic proteins,[8; 9] the latter of which become trapped in the vesicle lumen during release from the cell surface. OMVs are largely devoid of inner membrane and cytoplasm components although several studies indicate that chromosomal, phage and plasmid DNA can infiltrate OMVs as a means of OMV-mediated transfer of genetic information between bacteria.[10; 11; 12; 13]

An intriguing yet poorly understood phenomena pertaining to OMVs is the observation that certain membrane and/or soluble periplasmic proteins are enriched in vesicles while others are preferentially excluded. The majority of these enriched proteins happen to be virulence factors including, for example, *Escherichia coli* cytolysin A (ClyA),[14] enterotoxigenic *E. coli* heat labile enterotoxin (LT),[8] and *Actinobacillus actinomycetemcomitans* leukotoxin,[15] whereas proteins that are excluded from OMVs include numerous unidentified outer membrane (OM) proteins[15] as well as *E. coli* DsbA.[14] The preferential exclusion of proteins raises the interesting possibility that a yet-to-be determined sorting mechanism exists in the bacterial periplasm for discriminatory loading of a highly specific subset of proteins into OMVs.[14; 16] Moreover, the observation that certain virulence factors are enriched in vesicles suggests that OMVs may play a key role in bacterial pathogenesis by mediating transmission of active virulence factors and other bacterial envelope components to host cells. Indeed, numerous vesicle-associated virulence factors (e.g., adhesins, immunomodulatory compounds, proteases and toxins) have been shown to induce cytotoxicity, confer vesicle binding to and invasion of host cells, and modulate the host immune response.[8; 17; 18; 19; 20]

To date, one of the best studied vesicle-associated virulence factors is the 34-kDa cytotoxin ClyA (also called HlyE or SheA) found in pathogenic and non-pathogenic *E. coli* strains [14; 21] and also in *Salmonella enterica* serovars Typhi and Paratyphi A.[22] Structural studies indicate that the water-soluble form of ClyA is a bundle of four major α-helices, with a small surface-exposed hydrophobic beta-hairpin at the “head” end of the structure, and the N- and C-termini at the “tail” end[23] while lipid-associated ClyA forms an oligomeric pore complex comprised of either 8 or 13 ClyA subunits.[24; 25] Expression of the *clyA* gene is silenced in non-pathogenic *E. coli* K-12 laboratory strains by the nucleoid protein H-NS[26] but is derepressed in H-NS-deficient *E. coli*, thereby inducing cytotoxicity towards cultured mammalian cells.[27] More recent evidence indicates that ClyA is exported from *E. coli* in OMVs and retains a cytolytically active, oligomeric conformation in the vesicles.[14] However, the route by which ClyA manages to cross the bacterial IM and assemble in OMVs remains a mystery, as it carries no canonical signal peptide[21] and is not N-terminally processed.[28] Also undetermined is the role that ClyA plays in vesicle-mediated interactions with mammalian cells. Thus, in the present study, we sought to engineer synthetic membrane vesicles (s-MVs) with non-native functions that could be used for a wide range of applications including, for instance, the analysis of the complete ClyA translocation process. Specifically, we have programmed s-MVs with enhanced functionality by creating chimeras

between heterologous proteins such as green fluorescent protein (GFP) or β-lactamase (Bla) and ClyA. Using these engineered vesicles, we have determined that ClyA is capable of co-localizing a variety of structurally diverse fusion partners to the surface of *E. coli* and their released vesicles, but only when the periplasmic disulfide bond-forming machinery was present. Importantly, these cell- and OMV-associated proteins retained their biological activity, suggesting that the functionality of natural OMVs can be easily expanded via the expression of ClyA chimeras.

Results

GFP co-localizes in outer membrane vesicles when fused to ClyA

Previous studies demonstrated that genetic fusions between *E. coli* ClyA and reporter proteins such as Bla and GFP were efficiently translocated across the cytoplasmic membrane[29; 30] and that localization was independent of the position (N- or C-terminus) of ClyA in the fusion protein.[29] Separately, Wai and coworkers demonstrated that ClyA was exported from laboratory strains of *E. coli* cells via OMVs composed of outer membrane and periplasm.[31] These same authors reported that ClyA was significantly enriched in OMVs relative to other lumenal and membrane-bound OMV proteins.[14] Based on these results, we hypothesized that proteins fused to the N- or C-terminus of ClyA would be efficiently co-localized in OMVs and would retain their native function following vesicle localization. To test this, we first generated fusion constructs between GFP and the N- or C-terminus of ClyA. Expression of these fusion proteins in the OMV hyper-producing strain JC8031[32] followed by purification of vesicles from cell-free culture supernatants yielded uniform s-MVs (Fig. 1a) with an average diameter (Fig. 1b) and zeta-potential (data not shown) that were nearly indistinguishable from naked OMVs produced from plasmid-free JC8031 cells. This result was consistent with earlier findings that vesicle density and size were unaltered due to the incorporation of a heterologous vesicle protein.[33] A significant level of ClyA-GFP or GFP-ClyA was localized in vesicles whereas unfused GFP expressed alone was not detected in the s-MV preparations (Fig. 1c). Consistent with earlier studies of ClyA localization,[14; 31] subcellular fractionation of *E. coli* cells revealed that unfused ClyA accumulated in the cytoplasm, periplasm and OMV fractions (Fig. 1d). Likewise, the addition of GFP as an N- or C-terminal passenger protein resulted in a similar pattern of localization (Fig. 1d), although the amount of ClyA fusions in the insoluble fraction clearly increased compared to unfused ClyA (data not shown). Both fusion proteins were fluorescent in the cytoplasm, periplasm, and OMV fractions (Fig. 1e and f) and the whole cell fluorescence associated with cells expressing ClyA-GFP or GFP-ClyA was nearly as bright as cells expressing GFP alone (data not shown). Taken together, the data clearly indicate that GFP was compatible with ClyA translocation as chimeras between these two proteins co-localized in OMVs without significant losses in fluorescence activity.

The quality of the fractionation procedure was confirmed by the observation that endogenously expressed outer membrane protein OmpA was always found predominantly in the OMV fraction (shown for cells expressing ClyA-GFP, Fig. 1d), consistent with earlier studies,[14] while GroEL was found exclusively in the cytoplasmic fraction (data not shown) and DsbA in the periplasmic fraction (Fig. 1d). In our hands, DsbA also accumulated to high

levels in the OMV fraction (Fig. 1d). While it is common for periplasmic proteins to become entrapped in OMVs,[8; 9; 14; 33] the presence of DsbA was unexpected based on the findings of Wai and coworkers who reported that this protein was excluded from their OMV fractions.[14] One explanation for this discrepancy might have been our use of the *tolRA* mutant strain JC8031, which despite its tendency to secrete copious amounts of vesicles is also characterized by a leaky outer membrane.[32; 34] However, similar patterns of ClyA-GFP and DsbA localization were observed following subcellular fractionation of Δ*nlpI* mutant cells (Fig. 1d) that is known to produce relatively large quantities of vesicles but does not exhibit membrane instability.[34] Thus, the explanation that we currently favor, based on earlier observations,[8] is that our use of a different host strain resulted in altered vesicle protein profiles.

To determine whether ClyA-GFP in the pelleted supernatant was associated with intact vesicles and not with released outer membrane fragments, we next tested whether the fusion protein co-migrated with both periplasmic and outer membrane material. To this end, pelleted supernatant from cells expressing ClyA-GFP was separated by density gradient centrifugation. Western blotting and densitometry analysis of the resulting fractions revealed a gradient profile for ClyA-GFP that peaked in fractions 6–8 (Fig. 2a and b), reminiscent of the gradient profile of OMV-associated α-hemolysin.[35] As expected, the maximal GFP activity was detected in the same fractions that contained the ClyA-GFP-enriched OMVs (Fig. 2b and c) although weaker fluorescence could be detected in denser fractions (Fig. 2c). The outer membrane protein OmpA was similarly enriched in fractions 6–8 containing the majority of the ClyA-GFP, but strong bands also appeared in fractions 9 and 10 (Fig. 2a). Interestingly, DsbA was more evenly distributed between fractions 5–10 (Fig. 2a), indicating co-migration with vesicles that included a large portion of ClyA-GFP (fractions 6–8) as well as with vesicles that contained lesser amounts of ClyA-GFP (fractions 5, 9 and 10).

ClyA anchors correctly folded GFP to the outer surface of *E. coli* and to the surface of s-MVs

To determine the topology of the ClyA-GFP and GFP-ClyA chimeras, we probed the surface accessibility of GFP on whole cells and on vesicles. Previous studies showed that a fraction of the secreted ClyA remains located on the bacterial cell surface.[14] Likewise, we observed that both ClyA-GFP and GFP-ClyA were localized to the cell surface as evidenced by the accessibility of the GFP moiety to cross-reacting antibodies. Specifically, positive immunofluorescent- and immunogold-labeling using anti-GFP antibodies was detected for JC8031 cells expressing ClyA fused with GFP but not in the cases of unfused ClyA or unfused GFP (Fig. 3, shown for unfused GFP and ClyA-GFP).

To determine if the GFP associated with vesicles was similarly accessible to cross-reacting antibodies, immunofluorescent labeling of s-MVs was performed but only a weak immunofluorescent signal above background could be seen in this analysis (data not shown). This prompted us to explore a more sensitive and quantitative surface plasmon resonance (SPR)-based strategy for detecting vesicle-associated GFP. For this, biotinylated anti-*E. coli* antibodies (test channel) and bovine serum albumin (BSA, reference channel) were coupled

to an SPR sensor chip through streptavidin binding. To verify that the SPR surface could capture our s-MVs, we introduced solutions containing varying amounts of intact s-MVs from fraction 7 above, where the initial concentration of s-MVs in this fraction was 13.5 ± 1.34 μg/μl. Following introduction of ClyA-GFP-containing s-MVs to the SPR, we immediately noticed that the test channel coated with anti-*E. coli* antibodies but not the BSA-coated reference channel was highly fluorescent (Fig. 4a), even after several PBS wash steps, indicating specific capture of our s-MVs on the SPR surface. SPR binding revealed concentration-dependent shifts in the SPR wavelength over a range of s-MV concentrations (0.02–0.70 μg/μl) (Fig. 4b and c). Importantly, there was no measurable change in SPR wavelength upon treatment of surface-captured s-MVs with PBS (data not shown), indicating that the fluorescent vesicles were stably and tightly bound to the immobilized anti-*E. coli* antibody. Finally, to determine whether our SPR strategy was suitable for detecting OMV-associated antigens, we introduced anti-GFP monoclonal antibodies into the test channel that contained surface-captured s-MVs displaying active GFP. Specific binding between anti-GFP antibodies and vesicle-associated GFP was confirmed by a marked increase in the SPR wavelength in the test channel (Fig. 4d, black line). Controls were performed where these s-MVs were treated with non-specific anti-His6× monoclonal antibodies or where s-MVs displaying unfused ClyA were captured on the SPR surface and treated with anti-GFP antibodies; both cases resulted in no detectable increase in the SPR wavelength (shown for anti-His6× treatment of Cly-GFP s-MVs in Fig. 4d, gray line).

We next performed Proteinase K (PK) susceptibility assays on ClyA-GFP and GFP-ClyA vesicles to determine whether the immuno-accessible GFP was protected by the vesicle structure. When s-MVs derived from JC8031 cells expressing ClyA-GFP or GFP-ClyA were incubated with PK in the absence of membrane-disrupting detergent, vesicle-associated fluorescence was completely abolished (Fig. 5a, shown for ClyA-GFP) suggesting that the majority of the functional GFP was surface exposed and not protected by the vesicle structure. Consistent with this, Western blot analysis confirmed that nearly all of the s-MV-associated ClyA-GFP was degraded to a lower molecular weight anti-GFP or anti-ClyA cross-reacting species upon treatment with PK (Fig. 5b, lanes 1–3 and 7–9). Interestingly, we observed a significant amount of PK-resistant material following identical treatment of GFP-ClyA s-MVs (Fig. 5b, lanes 4–6 and 10–12) that persisted even after incubation with 2–5× higher PK concentrations for 2× longer durations (data not shown). Since these PK-treated s-MVs were non-fluorescent but contained a considerable portion of PK-resistant GFP-ClyA, we conclude that only a fraction of the fusion localizes with functional GFP tethered outside the OMV while the remainder adopts an inactive conformation that is protected by the vesicle structure. Possible reasons for this include a localization defect caused by the relatively high level of expression for GFP-ClyA compared to ClyA-GFP and/or the apparent instability of the fusion as evidenced by the multiple anti-ClyA cross-reacting bands seen in the absence of PK (Fig. 5b, lane 10). For both chimeras, complete proteolytic digestion of GFP by PK occurred when membranes were disrupted by the addition of 1% SDS (Fig. 5b). Control experiments using purified, soluble ClyA-GFP showed that the protein was PK-sensitive both in the presence or absence of the detergent (data not shown).

Periplasmic disulfide bond-forming machinery is required for localization of ClyA and ClyA fusions in OMVs

In previous work, ClyA in the periplasm was shown to adopt a monomeric conformation owing to an intramolecular disulfide bond formed between the cysteine residues at positions 87 and 285 in the polypeptide.[36] The presence of the disulfide bond was sufficient to prevent oligomerization of ClyA and inactivate its native haemolytic activity. In agreement with this finding, Wai *et al*. reported that DsbA, the enzyme responsible for catalyzing the formation of disulfide bonds in periplasmic proteins, was absent from OMVs containing ClyA and that the absence of DsbA was necessary for ClyA to oligomerize into its haemolytic conformation.[14] Contrary to the findings of Wai *et al*., we found that DsbA was co-localized in vesicles containing the ClyA fusions (see Fig. 1 above). Thus, we hypothesized that oxidized, monomeric ClyA might be favorable for efficient cell surface and vesicle localization of our fusions. To test our hypothesis, we compared expression of ClyA-GFP in strain JC8031 and an isogenic *dsbA*::Kan mutant derived from JC8031. Western blot analysis revealed that while both strains accumulated similar amounts of ClyA-GFP in the periplasm, only in cells with DsbA present was localization of ClyA-GFP observed (Fig. 5c). This was corroborated by a complete lack of fluorescence seen for OMVs derived from JC8031 *dsbA*::Kan cells expressing ClyA-GFP (Fig. 5d). Immunofluorescent staining of these same cells revealed that localization of ClyA-GFP to the bacterial cell surface was also dependent upon DsbA (Fig. 5d). To our surprise, DsbA-dependent vesicle localization was also observed for unfused ClyA suggesting that the periplasmic redox state is a critical factor in regulating the efficiency of protein localization into vesicles under the conditions tested here. Interestingly, we observed very little, to no, apparent cytotoxicity for naked OMVs from plasmid-free JC8031 cells, consistent with earlier studies,[14] and also for s-MVs containing ClyA-His6, ClyA-GFP or GFP-ClyA (data not shown) suggesting that ClyA in our vesicles was not in its haemolytically-active, oligomeric conformation.

Engineered ClyA-GFP s-MVs are useful for visualizing vesicle interactions with eukaryotic cells

Previous studies have shown that vesicles derived from pathogenic *E. coli* or non-pathogenic *E. coli* strains can associate with eukaryotic cells.[20; 33] Thus, we next investigated whether s-MVs functionalized with ClyA-GFP were suitable for tracking vesicle association with eukaryotic cells. Previous attempts at this focused on loading GFP into the lumen of vesicles following its transport into the periplasm by the twin-arginine translocation (Tat) pathway.[33] However, GFP-containing OMVs were only weakly fluorescent and could not be tracked in host cells by microscopy, likely due to the low yield of GFP transport to the periplasm via the Tat system. To determine if s-MVs engineered with ClyA-GFP were bright enough for tracking studies, we performed vesicle-host cell co-incubation assays. Punctate green staining was observed following a 30 min incubation of HeLa cells with ~150 μg vesicles purified ClyA-GFP s-MVs and the intensity of this staining increased as the incubation time between HeLa cells and ClyA-GFP s-MVs increased (Fig. 6a). These results imply that vesicles persisted on the cell surface or had fused directly to the target cell membrane. To corroborate this, HeLa cells that had been incubated with purified ClyA-GFP-containing s-MVs were stained with a fluorescent version of the cell surface marker wheat germ

agglutinin (WGA) and then washed with PBS. Confocal microscopy revealed that ClyA-GFP OMVs co-localized with WGA on the exterior of the cell (data not shown). Next, we explored the fate of ClyA-GFP vesicles by examining whether the appearance of punctate fluorescence was temperature dependent, a hallmark of cellular internalization.[20; 37] HeLa cells incubated with vesicles containing ClyA-GFP at 4°C exhibited very low levels of cell-associated fluorescence (compare Fig. 6b). However, when HeLa cells were incubated with ClyA-GFP s-MVs at 4°C for 3 h and then shifted to 37°C for 3 hr, strong cell fluorescence was observed (Fig. 6b), leaving open the possibility that some s-MVs may be internalized0 at 37°C. A key factor in endocytosis is ganglioside M1 (G_{M1}), which is a eukaryotic cell surface receptor for enterotoxins such as LT and cholera toxin (CT) and is required for endocytosis of LT-containing OMVs derived from non-pathogenic *E. coli*.[20] Therefore, we tested whether the observed fluorescence of HeLa cells incubated with ClyA-GFP s-MVs was G_{M1}-dependent. Indeed, fluorescence associated with HeLa cells was significantly decreased following incubation with purified ClyA-GFP s-MVs that had been pretreated with G_{M1} (Fig. 6c). Moreover, incubation with G_{M1}-treated vesicles resulted in a small number of large fluorescent clusters and much less punctate green fluorescence than was observed for HeLa cells incubated with untreated ClyA-GFP OMVs (Fig. 6c). Thus, it appears that G_{M1} cell surface receptors may play an important role in mediating interactions between HeLa cells and engineered vesicles. Finally, to assay the cytotoxic effect of vesicles on target cells, we analyzed how cultured HeLa cells were affected by equivalent amounts of different vesicle preparations. In general, vesicles containing ClyA-His6 or ClyA-GFP exhibited virtually no detectable cytotoxicity (Fig. 6d), consistent with a monomoric, DsbA+ conformation[14] for both ClyA and ClyA-GFP in our vesicles.

Heterologous proteins co-localized in s-MVs via ClyA retain their activity

To determine whether proteins other than GFP could be fused to ClyA while still retaining their function, we generated a series of N- and C-terminal fusions between ClyA and the following enzymes: β-lactamase (Bla), organophosphorus hydrolase (OPH) and β-galactosidase (LacZ). Similar to what was seen for GFP, ClyA-Bla resulted in localization of Bla to the surface of JC8031 cells and vesicles as determined using a nitrocefin hydrolysis assay (Table 1). Since Bla expressed in the cytoplasm was not localized to the cell surface or vesicles and since nitrocefin is relatively impermeable to the outer membrane,[38; 39] these data provide strong evidence that the Bla moiety was externally localized on cells and vesicles. Similar results were obtained using the Bla substrate penicillin-G (data not shown), which also penetrates the outer membrane very poorly.[40] Interestingly, as was seen above for the chimeras between ClyA and GFP, fusion of Bla to the N-terminus of ClyA resulted in a significantly lower level of Bla activity. Consistent with these results, fusion of ClyA to the N-terminus of the OPH enzyme conferred a significant level of OPH activity to the surface of cells and vesicles, whereas OPH-ClyA resulted in no measurable surface-associated OPH activity (Table 1). Since the OPH substrate paraoxon used in these experiments is membrane impermeable,[41] we conclude that ClyA-OPH is oriented with OPH externally bound to both cells and vesicles. Also, since OPH activity depends upon homodimer formation,[42] ClyA apparently tethers OPH in a conformation that allows for dimerization with a neighboring ClyA-OPH molecule. Finally, to determine if the ability to display multimeric enzymes is a general feature of ClyA-mediated surface exposure, we

constructed ClyA fusions to the homotetrameric LacZ enzyme from *E. coli*.[43] While expression of ClyA-LacZ resulted in strong cytoplasmic LacZ activity, there was no measurable LacZ activity on the surface of cells or their derived s-MVs (Table 1). In fact, there was no LacZ activity in the periplasm of cells expressing ClyA-LacZ (data not shown), consistent with the observation that the normally cytoplasmic LacZ protein contains sequences that hinder transport[44] usually leading to a misfolded, and thus inactive, protein.

Single-chain antibody fragments (scFv) have been successfully used to create artificial immunoliposomes for targeting of these vesicles and their payloads to specific cell types.[45] Along similar lines, we sought to create bacterial "immuno-MVs" by displaying scFv fragments on *E. coli*-derived vesicles. For these experiments, we made use of an scFv derived from the 26–10 monoclonal antibody that binds with high affinity ($KD = 0.9 \pm 0.2 \times 10–9\ M^{-1}$) to the cardiac glycoside digoxin (scFv.Dig).[46]; [47] Using a fluorescent conjugate of digoxin (Dig-BODIPY), we observed that expression of ClyA-scFv.Dig, but not scFv.Dig alone, resulted in cells and vesicles that were able to bind the fluorescent probe (Fig. 7a). Since Dig-BODIPY cannot permeate the outer membrane under standard conditions, the detection of Dig-BODIPY binding activity using intact cells indicates that scFvs were functionally displayed on the outer cell and vesicle surface. For comparison, cells expressing scFv.Dig fused to the well-characterized Lpp-OmpA hybrid OM anchor[47] displayed uniform but notably weaker cell surface fluorescence and no detectable fluorescence on OMVs (Fig. 7a) despite the fact that wildtype OmpA localizes in OMVs (see also Fig. 1d above).

Lastly, we sought to determine if the capture of Dig-BODIPY by ClyA-scFv.Dig could be used as a genetic screen for ClyA localization. Consistent with the fluorescence microscopy results above, labeling of JC8031 cells expressing ClyA-scFv.Dig with Dig-BODIPY resulted in highly fluorescent cells as revealed by flow cytometry (Fig. 7b). However, when ClyA-scFv.Dig was expressed in JC8031 *dsbA*::Kan cells, fluorescence was completely abolished. Likewise, when scFv.Dig was expressed alone, as an N-terminal fusion to ClyA (scFv.Dig-ClyA), or as a C-terminal fusion to ClyA variants carrying mutations that were previously reported to disrupt translocation (e.g., deletion of 10–147 of the last C-terminal amino acids[31] or substitution of the Tyr288 residue with Gly[29]), no measurable cell fluorescence was detected (Fig. 7b).

Discussion

This work describes the development and characterization of engineered synthetic membrane vesicles (s-MVs) created by genetic fusion of a recombinant polypeptide with the *E. coli* cytotoxin ClyA. In general, it was observed that most recombinant polypeptide fusions co-localized with ClyA to the bacterial cell surface and into OMVs. Specifically, we demonstrated that direct fusion of Bla, OPH, GFP and anti-digoxin scFv to the C-terminus of ClyA resulted in functional display of each protein on the surface of *E. coli* cells and their derived OMVs, giving rise to s-MVs with significantly expanded, non-native functionality (e.g., fluorescence, antigen binding). Interestingly, fusion of each of these proteins to the N-terminus of ClyA yielded unpredictable results. For instance, scFv.Dig-ClyA exhibited no detectable activity on the surface of cells or OMVs while GFP-ClyA resulted in the display of active protein. In the latter case, even though a portion of the fusions was active, a

significant amount of non-fluorescent GFP-ClyA accumulated in OMVs. We also found that fusion of the enzymes Bla and OPH resulted in little to no activity on cells and OMVs when each enzyme was fused to the N-terminus of ClyA. These results are consistent with earlier studies where a 2-fold increase in secretion to the extracellular medium was observed for ClyA-Bla versus Bla-ClyA.[29] At present, it is not known why N-terminal fusions to ClyA were inconsisten whereas C-terminal fusions invariably yielded well-displayed proteins that retain their biological function. Our results might be explained by inspection of the medium-resolution structure of membrane-bound ClyA showing that the C-terminus of ClyA is embedded deeper within membranes (i.e., closer to the outer surface) than the N-terminal portion, which occurs close to the periplasmic side of the outer membrane.[24; 25] According to this model, fusions to the C-terminus of ClyA are closer to the outer surface and more likely to extend into the extracellular environment, especially with the addition of a flexible 5-residue Gly linker that was included in all of our fusions.

Based on its relative plasticity as a fusion partner, we expect ClyA to serve as a useful tethering module for: (1) dissecting the complete ClyA translocation pathway from bacteria to target host cells; and (2) biotechnological applications that rely on cell or OMV surface display, such as affinity maturation of antibody fragments and vaccine adjuvant development.[46; 47; 49; 50] For instance, with respect to genetic analysis, expression of ClyA-GFP and ClyA-scFv.Dig both proved capable of reporting the localization of ClyA to the bacterial cell surface and into OMVs and revealed an essential role for DsbA in the translocation process. A simple model for ClyA assembly in vesicles proposed by Uhlin and coworkers, and supported by our findings, is that ClyA oligomerization and membrane insertion is governed by the redox state of ClyA.[14] Here, however, we show that a more reducing environment in the periplasm, such as occurs when DsbA is absent, favors the localization of ClyA and ClyA fusions into vesicles. While the involvement of DsbA appears to be via direct oxidation of ClyA,[14] we cannot rule out the possibility that DsbA is responsible for the oxidation of a periplasmic or membrane component(s) that mediate the localization of ClyA and/or the formation of OMVs.

With respect to biotechnology, the ability of ClyA to anchor and functionally display a variety of different prokaryotic and eukaryotic proteins on the surface of bacterial cells and vesicles should be useful for numerous applications. First, ClyA exhibits properties that make it an ideal carrier protein for bacterial cell surface display of peptides and proteins and compares favorably with the well-established Lpp-OmpA surface anchor as evidenced by scFv binding of fluorescently tagged digoxin. Second, by judicious selection and display of specific scFv fragments on OMVs, one might be able to redirect these engineered “immuno-MVs” to specific cell types, or otherwise engineer the host-vesicle interaction, in order to achieve a desired therapeutic or immunological response. Along these lines, we provide encouraging data that engineered vesicles retain their characteristic interactions with mammalian cells[20; 33] and are almost completely non-cytotoxic. It is also noteworthy that expression of all ClyA fusions in this study had no measurable effect on the growth rate of bacterial cells relative to cells expressing unfused ClyA or empty vector controls, thus appreciable yields of cells or their derived OMVs should be attainable for any OMV-based application.

Materials and Methods

Bacterial Strains, Plasmids and Growth Conditions

The bacterial strains and plasmids used in this study are described in Table 2. Strain JCA were made by introducing the *dsbA*::Kan allele into JC8031 cells by P1 *vir* transduction using DHA as the donor. Plasmid pClyA was constructed by ligating the PCR-amplified *clyA* gene into pBAD18-Cm between *Sac*I and *Xba*I sites. Insertion of DNA encoding either the *gfpmut2* gene[51; 52] or a 6× polyhistidine sequence between *Xba*I and *Hin*dIII sites resulted in plasmids pGFP-ClyA and pClyA-His6, respectively. Plasmid pGFP-ClyA was constructed by first cloning the *gfpmut2* gene between *Sac*I and *Xma*I sites of pBAD18-Cm followed by insertion of the *clyA* gene between *Xma*I and *Xba*I sites. Plasmid pGFP was constructed by ligating the PCR-amplified *gfpmut2* gene between *Sac*I and *Hin*dIII sites of pBAD18-Cm. For ClyA-X fusions in pBAD24, each of the PCR-amplified partner genes (except for *bla*) was inserted between *Xma*I and *Sph*I sites followed by *clyA* ligation between *Nco*I and *Xma*I sites. X-ClyA fusions were similarly constructed in pBAD24 with the ligations of fusion partner between *Nco*I and *Xma*I, and *clyA* between *Xma*I and *Sph*I. Control plasmids without *clyA* were constructed by inserting the fusion partner, X, between *Nco*I and *Sph*I of pBAD24. For Bla fusions with ClyA, a similar strategy as described above was used for inserting *clyA* and *bla* into plasmid pBAD18-Kan between *Sac*I and *Xma*I and *Sph*I sites. The gene encoding the Lpp-OmpA-scFv.Dig chimera in pB18D was amplified and ligated into pBAD24 between *Nco*I and *Sph*I, resulting in pB24D. To generate pClyA(Δ156–303)-scFv.Dig, pClyA-scFv.Dig was digested with *Hpa*I and *Xma*I and then self-ligated via blunt-end ligation after removal of overhanging basepairs. To generate pClyA(Δ293–303)-scFv.Dig, DNA encoding the first 292 amino acids of ClyA was PCR-amplified and inserted in place of wt *clyA* in pClyA-scFv.Dig. Plasmid pClyA(Y288G)-scFv.Dig was generated with pClyA-scFv.Dig as template for site-directed mutagenesis using a Stratagene QuickChange® site-directed mutagenesis kit. Cells were grown in LB broth with appropriate antibiotics: ampicillin, 100 μg/ml; chloramphenicol, 25 μg/ml; and kanamycin, 50 μg/ml. Cell growth was maintained at 37°C unless otherwise noted. Protein synthesis was induced for 6 h by adding 0.2% arabinose when cells reached an $OD_{600} \approx 0.5$.

Cell culture

Human epithelial cervical carcinoma (HeLa) cells were obtained from the American Type Culture Collection (ATCC # CCL-2) and grown in Dulbecco's modified Eagle's minimal essential medium (DMEM) supplemented with 10% NuSerum, and 1% penicillin/streptomycin. Cells were maintained at 37°C in a humidified atmosphere of 95% air, 5% CO_2. For fluorescence microscopy experiments, cells were grown on 12-mm circular glass coverslips for two days prior to experimentation.

Subcellular fractionation

Cytoplasmic and periplasmic fractions from cells expressing fusion proteins were generated by the cold osmotic shock procedure[53] and the pellet remaining after removal of the soluble fraction was collected as the insoluble fraction.

Isolation of bacterial vesicles

Vesicles were isolated from late log-phase bacterial cultures grown aerobically at 37°C in LB broth (unless otherwise indicated) essentially as described previously.[14] Briefly, bacterial cells were removed by centrifugation at 5,000×g for 15 min at 4°C and the cell-free supernatants were filtered through a 0.2 μm-pore-size vacuum filter. Vesicles were collected from the filtered supernatant by ultracentrifugation at 141,000×g for 2 h at 4 °C in a 28 Ti rotor (Beckman Instruments, Inc.) and the pellet containing OMVs was carefully removed and suspended in PBS (pH 7.0). Vesicle preparations were plated on LB agar to confirm complete removal of bacterial cells. Vesicles preparations were kept at −20°C.

Outer membrane vesicles fractionation

Separation of pelleted outer membrane vesicle samples was performed as described.[8] Briefly, vesicles were isolated as described above but suspended in 50 mM HEPES (pH 6.8), adjusted to 45% Optiprep (Sigma) in 0.15 ml and transferred to the bottom of 12-ml ultracentrifugation tubes. Different Optiprep/HEPES layers were sequentially added as follows: 0.9 ml 35%, 0.9 ml 30%, 0.66 ml 25%, 0.66 ml 20%, 0.33 ml 15% and 0.33 ml 10%. Gradients were centrifuged (180,000×g, 180 min, 4°C). A total of 10 fractions of equal volumes were sequentially removed and analysed by SDS-PAGE.

Vesicle characterization

The amount of vesicles in purified cell-free supernatant was determined by measuring the total protein concentration or the dry mass of vesicles according to published protocols.[54] Particle size distribution and zeta potential of vesicle samples containing approximately 30 μg/mL total protein in 1 mL of PBS were measured in a Nanosizer Nano ZS instrument (Malvern Instruments) using standard protocols. Malvern Dispersion Technology Software was used for data acquisition and analysis, applying the general purpose algorithm for calculating size distributions and the Smoluchowski approximation for determining zeta potential.

Protein assays

Whole cells, OMVs and subcellular fractions were assayed for Bla, LacZ and OPH activity using nitrocefin (Sigma), ONPG (Sigma) and paraoxon (Sigma), respectively, according to standard spectrophotometric assays.[55; 56; 57] Cells expressing anti-digoxin scFv were labeled with Dig-BODIPY and analyzed by flow cytometry as described.[58] Total protein concentration was assayed using the BCA Protein Assay kit (Pierce). Protease accessibility assays were performed as described but with Proteinase K.[33] Briefly, vesicles were treated at 37°C for 30 min in 20 mM Tris HCl (pH 8.0) with PK (0.1 mg/ml) in either the absence or presence of 1% SDS. In parallel control experiments, ClyA-GFP and GFP-ClyA that had been purified by IMAC were similarly treated with PK. Following the incubation, all samples were placed on ice and 1 mM PMSF was added to quench all proteolysis, and the samples were analysed by SDS-PAGE. Western blotting was performed as described by Chen *et al*.[48] using the following primary antibodies: anti-ClyA (kindly provided by Sun Nyunt Wai, Umeå University, Sweden), anti-GFP (Sigma), anti-GroEL (Sigma), anti-polyhistidine (Sigma), anti-OmpA and anti-DsbA (kindly provided by Jon Beckwith,

Harvard Medical School). Membranes were developed on film using Immuno-Star™ HRP Substrate Kit (Bio-Rad).

Surface plasmon resonance (SPR)

The SPR configuration consisted of a sensor chip, an optical measuring unit, a flow cell and a syringe pump and was similar to that developed previously.[59; 60] The SPR chip was SF10 glass with a thin layer (50 nm) of gold that was attached to a prism made of SF10 using index matching oil. Two microfluidic channels (reference and test) made of polydimethylsiloxane (PDMS) were placed on the SPR sensor chip and screw-clamped to seal the channels. Single-wavelength light was obtained by passing white light from a Xe-lamp (Oriel) through a monochromater (Oriel). Light with a bandwidth less than 1 nm passed through the polarizer, where only p-polarized light was transmitted. The reflected light intensity (RI) was measured with a CCD camera (Sony) that showed high sensitivity around 600 nm. When the incident angle of the beam was fixed to 60 degrees, treatment of the sensor chip with PBS resulted in an SPR wavelength of about 600 nm. The SPR wavelength was obtained at each pixel by fitting the RI versus wavelength data to a second-order polynomial equation and the resulting SPR wavelengths, covering a pre-defined region of interest, were averaged. Before each measurement, the RI of s-polarized light was recorded at each pixel for reference. The reliable detection limit of the SPR sensor was measured to be less than 0.2 nm.

Vesicle and vesicle antigen detection using SPR

An SPR chip for detection of vesicles and vesicle-associated antigens was performed as follows. First, an alkanethiol monolayer was self-assembled on the 50-nm gold layer of the sensor chip surface with a mixed solution (1:2 molar ratio) of 10 mM 11-mercaptoundecanoic acid (11-MUA) and 6-mercapto-1-hexanol (6-MCH) as described previously.[61; 62] The hydroxyl-terminated self-assembled monolayer (SAM), which cannot be activated by *N*-hydroxysuccinimide (NHS) and *N*-ethyl-*N*'-(3-diethylaminopropyl) carbodiimide (EDC), was used as a spacer to construct the sensor surface. Second, following activation of the terminal carboxylic groups of the mixed SAM with a 1:1 mixture of 0.1 M NHS and 0.4 M EDC for 10 min, streptavidin (SA; 200 μg/ml; MP Biomedicals) in 10 mM sodium acetate buffer (pH 5.5) was injected and allowed to covalently couple for 15–20 min followed by PBS rinsing and blocking with 1.0 M ethanolamine hydrochloride (pH 8.5) for 10 min. This resulted in a large increase in the SPR wavelength (data not shown). Because of the close relationship that exists between electrostatic binding and covalent binding of SA with carboxylic terminated SAMs, this increase in SPR signal is a decent estimate of the extent of covalent binding of SA to the SAMs.[61] Third, following a thorough PBS wash, biotinylated rabbit anti-*E. coli* antibody (140 μg/ml in PBS; Cortex Biochem) was injected over the SA surface for 20 min and unbound biotinylated anti-*E. coli* antibody was removed by washing with PBS for 10 min. This resulted in an exponential increase in the SPR wavelength that was characteristic of electrostatic binding between SA and biotin-conjugated proteins (data not shown). As control, bovine serum albumin (BSA; 140 μg/ml in sodium acetate buffer) was added in place of anti-*E. coli* antibody to the SA-coated reference channel of the SPR sensor chip and, as expected, no detectable SPR wavelength

shift was observed following introduction of BSA or, subsequently, anti-*E. coli* antibody (data not shown).

Fluorescence microscopy

For immunofluorescence studies, *E. coli* cells that had been induced to express GFP or ClyA-GFP were washed three times in PBS, incubated at 4°C overnight with mouse anti-GFP (or anti-polyhistidine) diluted 1:500, pelleted, washed three times with PBS, incubated for 1 h with rhodamine-labeled goat anti-mouse IgG (Molecular Probes) diluted 1:100, pelleted and washed three more times with PBS. Finally, cells were examined by a Zeiss Axioskop 40 fluorescent microscope with Spotflex color digital camera and filter sets for GFP (485 nm for excitation and 505 nm for emission) and Rhodamine (540 nm for excitation and 600 nm for emission). For fluorescent studies of OMV interactions with eukaryotic cells, HeLa cells grown on glass coverslips were washed in OptiMEM (Life Technologies) without serum and then treated as described under Results. Following treatment, cells were fixed with 3.7% formalin in PBS, washed three times in PBS, permeabilized in PBS/0.1% Triton X-100, stained with 0.5 mg/mL ethidium bromide in PBS, and finally washed three times in PBS. Coverslips were mounted onto glass slides using Vectashield Hardset mounting medium (Vector Laboratories) prior to wide-field epifluorescence analysis. For WGA studies, non-permeabilized cells were incubated with 1 μg/ml Texas red WGA (Molecular Probes) for 1 h at 4°C. For G_{M1} experiments, ~150 μg of vesicles were preincubated with 10 μg G_{M1} (Sigma) for 30 min at 25°C.

Electron microscopy

Ultrastructural analysis of vesicles was performed by negative staining technique as described previously.[63] For immunogold labeling, a 10-μL suspension of induced *E. coli* cells was collected, washed and applied to 400-mesh Formvar- and carbon-coated copper grids (Electron Microscopy Sciences) and incubated for 1 h with anti-GFP diluted 1:500. Cells were washed with PBS, incubated for 1 h with 25 nm colloidal gold-conjugated goat anti-mouse IgG (Electron Microscopy Sciences) diluted 1:100, washed again, negatively stained with 0.25% phosphotungstic acid (PTA, Electron Microscopy Sciences) with 0.01% BSA in water and viewed using a FEI/Philips Morgagni transmission electron microscope.

Cytotoxicity assay

Vesicles were prepared in PBS and total protein in vesicle fractions was quantified by the Coomassie Plus Assay (Pierce) using BSA protein standards. HeLa cells were grown in clear, flat-bottom tissue culture polystyrene 96-well plates (Costar) at an initial density of 5,000 cells per well in 200 μL of growth medium. After 24 h, the growth medium was removed and replaced with 110 μL of Opti-MEM I® (Invitrogen) serum-free medium and 40 μL of undiluted (1×; ~90–150 μg/ml total protein) or 1:1 diluted (0.5×; ~40–60 μg/ml total protein) OMV samples in PBS. Cells were incubated in the presence of vesicle samples for 4 h; afterwards the OMV-containing medium was removed and replaced with 175 μL of phenol red-free growth medium. Following an additional 48 h of incubation, 35 μL of CellTiter 96® Aqueous One Solution Cell Proliferation Assay reagent (Promega) was added to the wells. This assay uses the tetrazolium compound [3-(4,5-dimethylthiazol-2-yl)-5-(3-

carboxymethoxyphenyl)-2-(4-sulfophenyl)-2H–tetrazolium, inner salt; MTS] and the electron coupling reagent phenazine methosulfate. MTS is chemically reduced by cells into formazan whose concentration and optical absorbance at 490 nm provide a measure of metabolically active live cells. Samples were incubated for 1 h and the absorbance was read in a microplate spectrophotometer at 490 nm. Cell viability is reported relative to PBS controls.

Acknowledgements

We thank Kyung Hun Yoonand Michael Shuler (Cornell University) and Sang Hun Lee, Tai Hyun Park and Sung June Kim (Seoul National University) for their assistance with the SPR studies. We also thank Harris Bernstein, Wilfred Chen, George Georgiou, Koreaki Ito, Roland Lloubes, Virginia Miller, Sun Nyunt Wai and Joel Weiner for their generous gifts of strains, plasmids and antibodies. This material is based upon work supported by the Ladies Auxiliary to the Veterans of Foreign Wars Cancer Research Fellowship (to A.M.D.), a New York State Health Research Science Board (HRSB) Breast Cancer Research Fellowship (to A.M.D.), the National Institutes of Health under Grant R21 NIBIB EB005669 (to D.A.P. and M.P.D), and a NYSTAR James D. Watson Young Investigator Award (to M.P.D.).

References

1. Christie PJ, Vogel JP. Bacterial type IV secretion: conjugation systems adapted to deliver effector molecules to host cells. Trends Microbiol. 2000; 8:354–360. [PubMed: 10920394]
2. Galan JE, Collmer A. Type III secretion machines: bacterial devices for protein delivery into host cells. Science. 1999; 284:1322–1328. [PubMed: 10334981]
3. Gentschev I, Dietrich G, Goebel W. The *E. coli* alpha-hemolysin secretion system and its use in vaccine development. Trends Microbiol. 2002; 10:39–45. [PubMed: 11755084]
4. Henderson IR, Cappello R, Nataro JP. Autotransporter proteins, evolution and redefining protein secretion. Trends Microbiol. 2000; 8:529–532. [PubMed: 11115743]
5. Russel M. Macromolecular assembly and secretion across the bacterial cell envelope: type II protein secretion systems. J Mol Biol. 1998; 279:485–499. [PubMed: 9641973]
6. Kuehn MJ, Kesty NC. Bacterial outer membrane vesicles and the host-pathogen interaction. Genes Dev. 2005; 19:2645–2655. [PubMed: 16291643]
7. Beveridge TJ. Structures of gram-negative cell walls and their derived membrane vesicles. J Bacteriol. 1999; 181:4725–4733. [PubMed: 10438737]
8. Horstman AL, Kuehn MJ. Enterotoxigenic *Escherichia coli* secretes active heat-labile enterotoxin via outer membrane vesicles. J Biol Chem. 2000; 275:12489–12496. [PubMed: 10777535]
9. McBroom, A.; Kuehn, MJ. Outer membrane vesicles. In: R, C., III, editor. EcoSal - Escherichia coli and Salmonella: Cellular and molecular biology. Washington, D.C.: ASM Press; 2005.
10. Dorward DW, Garon CF, Judd RC. Export and intercellular transfer of DNA via membrane blebs of *Neisseria gonorrhoeae*. J Bacteriol. 1989; 171:2499–2505. [PubMed: 2496108]
11. Kolling GL, Matthews KR. Export of virulence genes and Shiga toxin by membrane vesicles of *Escherichia coli* O157:H7. Appl Environ Microbiol. 1999; 65:1843–1848. [PubMed: 10223967]
12. Yaron S, Kolling GL, Simon L, Matthews KR. Vesicle-mediated transfer of virulence genes from *Escherichia coli* O157:H7 to other enteric bacteria. Appl Environ Microbiol. 2000; 66:4414–4420. [PubMed: 11010892]
13. Renelli M, Matias V, Lo RY, Beveridge TJ. DNA-containing membrane vesicles of *Pseudomonas aeruginosa* PAO1 and their genetic transformation potential. Microbiology. 2004; 150:2161–2169. [PubMed: 15256559]
14. Wai SN, Lindmark B, Soderblom T, Takade A, Westermark M, Oscarsson J, Jass J, Richter-Dahlfors A, Mizunoe Y, Uhlin BE. Vesicle-mediated export and assembly of pore-forming oligomers of the enterobacterial ClyA cytotoxin. Cell. 2003; 115:25–35. [PubMed: 14532000]

15. Kato S, Kowashi Y, Demuth DR. Outer membrane-like vesicles secreted by *Actinobacillus actinomycetemcomitans* are enriched in leukotoxin. Microb Pathog. 2002; 32:1–13. [PubMed: 11782116]
16. McBroom AJ, Kuehn MJ. Release of outer membrane vesicles by Gram-negative bacteria is a novel envelope stress response. Mol Microbiol. 2007; 63:545–558. [PubMed: 17163978]
17. Fiocca R, Necchi V, Sommi P, Ricci V, Telford J, Cover TL, Solcia E. Release of *Helicobacter pylori* vacuolating cytotoxin by both a specific secretion pathway and budding of outer membrane vesicles. Uptake of released toxin and vesicles by gastric epithelium. J Pathol. 1999; 188:220–226. [PubMed: 10398168]
18. Keenan J, Day T, Neal S, Cook B, Perez-Perez G, Allardyce R, Bagshaw P. A role for the bacterial outer membrane in the pathogenesis of *Helicobacter pylori* infection. FEMS Microbiol Lett. 2000; 182:259–264. [PubMed: 10620676]
19. Kadurugamuwa JL, Beveridge TJ. Delivery of the non-membrane-permeative antibiotic gentamicin into mammalian cells by using *Shigella flexneri* membrane vesicles. Antimicrob Agents Chemother. 1998; 42:1476–1483. [PubMed: 9624497]
20. Kesty NC, Mason KM, Reedy M, Miller SE, Kuehn MJ. Enterotoxigenic *Escherichia coli* vesicles target toxin delivery into mammalian cells. EMBO J. 2004; 23:4538–4549. [PubMed: 15549136]
21. del Castillo FJ, Leal SC, Moreno F, del Castillo I. The *Escherichia coli* K-12 sheA gene encodes a 34-kDa secreted haemolysin. Mol Microbiol. 1997; 25:107–115. [PubMed: 11902713]
22. Oscarsson J, Westermark M, Lofdahl S, Olsen B, Palmgren H, Mizunoe Y, Wai SN, Uhlin BE. Characterization of a pore-forming cytotoxin expressed by *Salmonella enterica* serovars typhi and paratyphi A. Infect Immun. 2002; 70:5759–5769. [PubMed: 12228306]
23. Wallace AJ, Stillman TJ, Atkins A, Jamieson SJ, Bullough PA, Green J, Artymiuk PJ. *E. coli* hemolysin E (HlyE, ClyA, SheA): X-ray crystal structure of the toxin and observation of membrane pores by electron microscopy. Cell. 2000; 100:265–276. [PubMed: 10660049]
24. Eifler N, Vetsch M, Gregorini M, Ringler P, Chami M, Philippsen A, Fritz A, Muller SA, Glockshuber R, Engel A, Grauschopf U. Cytotoxin ClyA from *Escherichia coli* assembles to a 13-meric pore independent of its redox-state. EMBO J. 2006; 25:2652–2661. [PubMed: 16688219]
25. Tzokov SB, Wyborn NR, Stillman TJ, Jamieson S, Czudnochowski N, Artymiuk PJ, Green J, Bullough PA. Structure of the hemolysin E (HlyE, ClyA, SheA) channel in its membrane-bound form. J Biol Chem. 2006; 281:23042–23049. [PubMed: 16754675]
26. Westermark M, Oscarsson J, Mizunoe Y, Urbonaviciene J, Uhlin BE. Silencing and activation of ClyA cytotoxin expression in *Escherichia coli*. J Bacteriol. 2000; 182:6347–6357. [PubMed: 11053378]
27. Gomez-Gomez JM, Blazquez J, Baquero F, Martinez JL. Hns mutant unveils the presence of a latent haemolytic activity in *Escherichia coli* K-12. Mol Microbiol. 1996; 19:909–910. [PubMed: 8820659]
28. Ludwig A, Bauer S, Benz R, Bergmann B, Goebel W. Analysis of the SlyA-controlled expression, subcellular localization and pore-forming activity of a 34 kDa haemolysin (ClyA) from *Escherichia coli* K-12. Mol Microbiol. 1999; 31:557–567. [PubMed: 10027972]
29. del Castillo FJ, Moreno F, del Castillo I. Secretion of the *Escherichia coli* K-12 SheA hemolysin is independent of its cytolytic activity. FEMS Microbiol Lett. 2001; 204:281–285. [PubMed: 11731136]
30. Galen JE, Zhao L, Chinchilla M, Wang JY, Pasetti MF, Green J, Levine MM. Adaptation of the endogenous *Salmonella enterica* serovar Typhi clyA-encoded hemolysin for antigen export enhances the immunogenicity of anthrax protective antigen domain 4 expressed by the attenuated live-vector vaccine strain CVD 908-htrA. Infect Immun. 2004; 72:7096–7106. [PubMed: 15557633]
31. Wai SN, Westermark M, Oscarsson J, Jass J, Maier E, Benz R, Uhlin BE. Characterization of dominantly negative mutant ClyA cytotoxin proteins in *Escherichia coli*. J Bacteriol. 2003; 185:5491–5499. [PubMed: 12949101]
32. Bernadac A, Gavioli M, Lazzaroni JC, Raina S, Lloubes R. *Escherichia coli tol-pal* mutants form outer membrane vesicles. J Bacteriol. 1998; 180:4872–4878. [PubMed: 9733690]

33. Kesty NC, Kuehn MJ. Incorporation of heterologous outer membrane and periplasmic proteins into *Escherichia coli* outer membrane vesicles. J Biol Chem. 2004; 279:2069–2076. [PubMed: 14578354]
34. McBroom AJ, Johnson AP, Vemulapalli S, Kuehn MJ. Outer membrane vesicle production by *Escherichia coli* is independent of membrane instability. J Bacteriol. 2006; 188:5385–5392. [PubMed: 16855227]
35. Balsalobre C, Silvan JM, Berglund S, Mizunoe Y, Uhlin BE, Wai SN. Release of the type I secreted alpha-haemolysin via outer membrane vesicles from *Escherichia coli*. Mol Microbiol. 2006; 59:99–112. [PubMed: 16359321]
36. Atkins A, Wyborn NR, Wallace AJ, Stillman TJ, Black LK, Fielding AB, Hisakado M, Artymiuk PJ, Green J. Structure-function relationships of a novel bacterial toxin, hemolysin E. The role of alpha G. J Biol Chem. 2000; 275:41150–41155. [PubMed: 11006277]
37. Pelkmans L, Kartenbeck J, Helenius A. Caveolar endocytosis of simian virus 40 reveals a new two-step vesicular-transport pathway to the ER. Nat Cell Biol. 2001; 3:473–483. [PubMed: 11331875]
38. Angus BL, Carey AM, Caron DA, Kropinski AM, Hancock RE. Outer membrane permeability in *Pseudomonas aeruginosa*: comparison of a wild-type with an antibiotic-supersusceptible mutant. Antimicrob Agents Chemother. 1982; 21:299–309. [PubMed: 6803666]
39. Good L, Sandberg R, Larsson O, Nielsen PE, Wahlestedt C. Antisense PNA effects in *Escherichia coli* are limited by the outer-membrane LPS layer. Microbiology. 2000; 146:2665–2670. [PubMed: 11021941]
40. Nikaido H, Normark S. Sensitivity of *Escherichia coli* to various beta-lactams is determined by the interplay of outer membrane permeability and degradation by periplasmic beta-lactamases: a quantitative predictive treatment. Mol Microbiol. 1987; 1:29–36. [PubMed: 3330755]
41. Richins RD, Kaneva I, Mulchandani A, Chen W. Biodegradation of organophosphorus pesticides by surface-expressed organophosphorus hydrolase. Nat Biotechnol. 1997; 15:984–987. [PubMed: 9335050]
42. Grimsley JK, Scholtz JM, Pace CN, Wild JR. Organophosphorus hydrolase is a remarkably stable enzyme that unfolds through a homodimeric intermediate. Biochemistry. 1997; 36:14366–14374. [PubMed: 9398154]
43. Jacobson RH, Zhang XJ, DuBose RF, Matthews BW. Three-dimensional structure of beta-galactosidase from *E. coli*. Nature. 1994; 369:761–766. [PubMed: 8008071]
44. Lee C, Li P, Inouye H, Brickman ER, Beckwith J. Genetic studies on the inability of beta-galactosidase to be translocated across the *Escherichia coli* cytoplasmic membrane. J Bacteriol. 1989; 171:4609–4616. [PubMed: 2527843]
45. Kontermann RE. Immunoliposomes for cancer therapy. Curr Opin Mol Ther. 2006; 8:39–45. [PubMed: 16506524]
46. Daugherty PS, Chen G, Iverson BL, Georgiou G. Quantitative analysis of the effect of the mutation frequency on the affinity maturation of single chain Fv antibodies. Proc Natl Acad Sci U S A. 2000; 97:2029–2034. [PubMed: 10688877]
47. Francisco JA, Campbell R, Iverson BL, Georgiou G. Production and fluorescence-activated cell sorting of *Escherichia coli* expressing a functional antibody fragment on the external surface. Proc Natl Acad Sci U S A. 1993; 90:10444–10448. [PubMed: 8248129]
48. Chen G, Hayhurst A, Thomas JG, Harvey BR, Iverson BL, Georgiou G. Isolation of high-affinity ligand-binding proteins by periplasmic expression with cytometric screening (PECS). Nat Biotechnol. 2001; 19:537–542. [PubMed: 11385457]
49. Chen W, Georgiou G. Cell-Surface display of heterologous proteins: From high-throughput screening to environmental applications. Biotechnol Bioeng. 2002; 79:496–503. [PubMed: 12209821]
50. Georgiou G, Stathopoulos C, Daugherty PS, Nayak AR, Iverson BL, Curtiss R 3rd. Display of heterologous proteins on the surface of microorganisms: from the screening of combinatorial libraries to live recombinant vaccines. Nat Biotechnol. 1997; 15:29–34. [PubMed: 9035102]
51. Crameri A, Whitehorn EA, Tate E, Stemmer WP. Improved green fluorescent protein by molecular evolution using DNA shuffling. Nat Biotechnol. 1996; 14:315–319. [PubMed: 9630892]

52. DeLisa MP, Samuelson P, Palmer T, Georgiou G. Genetic analysis of the twin arginine translocator secretion pathway in bacteria. J Biol Chem. 2002; 277:29825–29831. [PubMed: 12021272]

53. Kim JY, Fogarty EA, Lu FJ, Zhu H, Wheelock GD, Henderson LA, DeLisa MP. Twin-arginine translocation of active human tissue plasminogen activator in *Escherichia coli*. Applied and Environmental Microbiology. 2005; 71:8451–8459. [PubMed: 16332834]

54. Kadurugamuwa JL, Beveridge TJ. Virulence factors are released from *Pseudomonas aeruginosa* in association with membrane vesicles during normal growth and exposure to gentamicin: a novel mechanism of enzyme secretion. J Bacteriol. 1995; 177:3998–4008. [PubMed: 7608073]

55. Cho CM, Mulchandani A, Chen W. Bacterial cell surface display of organophosphorus hydrolase for selective screening of improved hydrolysis of organophosphate nerve agents. Appl Environ Microbiol. 2002; 68:2026–2030. [PubMed: 11916726]

56. Francisco JA, Earhart CF, Georgiou G. Transport and anchoring of beta-lactamase to the external surface of *Escherichia coli*. Proc Natl Acad Sci U S A. 1992; 89:2713–2717. [PubMed: 1557377]

57. Miller, JH. A Short Course in Bacterial Genetics. A Laboratory Manual and Handbook for Escherichia coli and Related Bacteria. Cold Spring Harbor, NY: Cold Spring Harbor Laboratory Press; 1992.

58. Daugherty PS, Olsen MJ, Iverson BL, Georgiou G. Development of an optimized expression system for the screening of antibody libraries displayed on the *Escherichia coli* surface. Protein Eng. 1999; 12:613–621. [PubMed: 10436088]

59. Baac H, Hajos JP, Lee J, Kim D, Kim SJ, Shuler ML. Antibody-based surface plasmon resonance detection of intact viral pathogen. Biotechnol Bioeng. 2006; 94:815–819. [PubMed: 16470580]

60. Ferracci G, Miquelis R, Kozaki S, Seagar M, Leveque C. Synaptic vesicle chips to assay botulinum neurotoxins. Biochem J. 2005; 391:659–666. [PubMed: 16011482]

61. Choi SH, Lee JW, Sim SJ. Enhanced performance of a surface plasmon resonance immunosensor for detecting Ab-GAD antibody based on the modified self-assembled monolayers. Biosens Bioelectron. 2005; 21:378–383. [PubMed: 16023966]

62. Lee JW, Sim SJ, Cho SM, Lee J. Characterization of a self-assembled monolayer of thiol on a gold surface and the fabrication of a biosensor chip based on surface plasmon resonance for detecting anti-GAD antibody. Biosens Bioelectron. 2005; 20:1422–1427. [PubMed: 15590298]

63. Wai SN, Takade A, Amako K. The release of outer membrane vesicles from the strains of enterotoxigenic *Escherichia coli*. Microbiol Immunol. 1995; 39:451–456. [PubMed: 8569529]

64. Datsenko KA, Wanner BL. One-step inactivation of chromosomal genes in *Escherichia coli* K-12 using PCR products. Proc Natl Acad Sci U S A. 2000; 97:6640–6645. [PubMed: 10829079]

65. Baba T, Ara T, Hasegawa M, Takai Y, Okumura Y, Baba M, Datsenko KA, Tomita M, Wanner BL, Mori H. Construction of *Escherichia coli* K-12 in-frame, single-gene knockout mutants: the Keio collection. Mol Syst Biol. 2006; 2:2006 0008.

66. Qi HY, Hyndman JB, Bernstein HD. DnaK promotes the selective export of outer membrane protein precursors in SecA-deficient *Escherichia coli*. J Biol Chem. 2002; 277:51077–51083. [PubMed: 12403776]

67. Guzman LM, Belin D, Carson MJ, Beckwith J. Tight regulation, modulation, and high-level expression by vectors containing the arabinose PBAD promoter. J Bacteriol. 1995; 177:4121–4130. [PubMed: 7608087]

68. Shimazu M, Mulchandani A, Chen W. Thermally triggered purification and immobilization of elastin-OPH fusions. Biotechnol Bioeng. 2003; 81:74–79. [PubMed: 12432583]

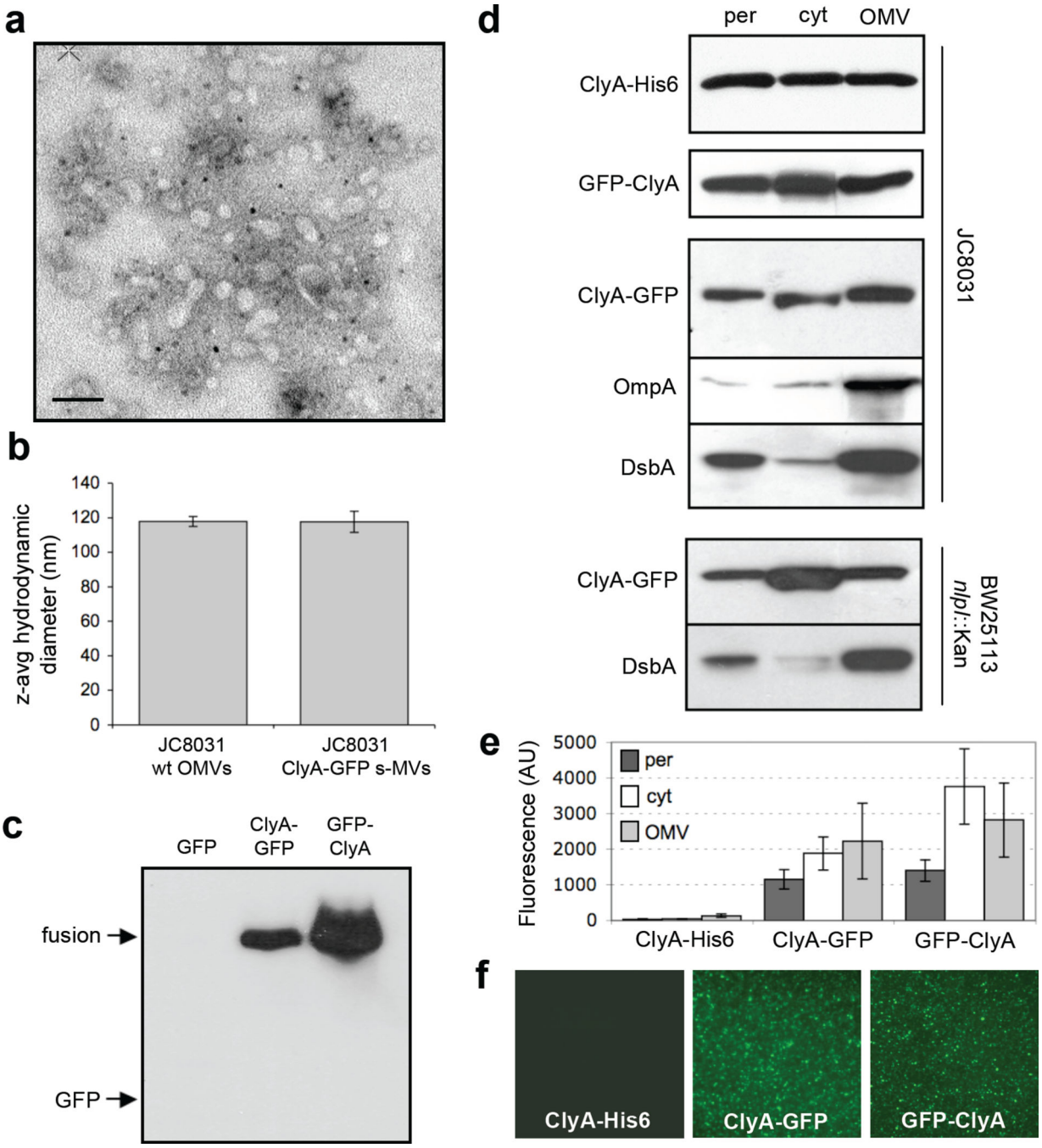

Figure 1.

Subcellular localization of ClyA and ClyA fusions. (a) Electron micrograph of vesicles derived from JC8031 cells expressing ClyA-GFP. Bar is equal to 100 nm. (b) Z-average particle size of 1 ml vesicle suspensions containing ~30 μg/ml total protein obtained from plasmid-free or ClyA-GFP-expressing JC8031 cells. Error bars represent the standard deviation of 3 replicates. (c) Western blot of vesicle fractions isolated from *E. coli* strain JC8031 expressing GFP, ClyA-GFP and GFP-ClyA. Blot was probed with anti-GFP serum. (d) Western blot and (e) GFP fluorescence of periplasmic (per), cytoplasmic (cyt) and

vesicle (OMV) fractions generated from JC8031 or BW25113 *nlpI*::Kan cells expressing ClyA-His6, ClyA-GFP and GFP-ClyA. ClyA-His6 blot was first probed with anti-polyhistidine. ClyA-GFP and GFP-ClyA blots were probed with anti-GFP. Following stripping of membranes, blots were reprobed with anti-OmpA serum or anti-DsbA serum as indicated. All fractions were generated from an equivalent number of cells. (f) Fluorescence microscopy of vesicles generated from JC8031 cells expressing ClyA-His6, ClyA-GFP and GFP-ClyA.

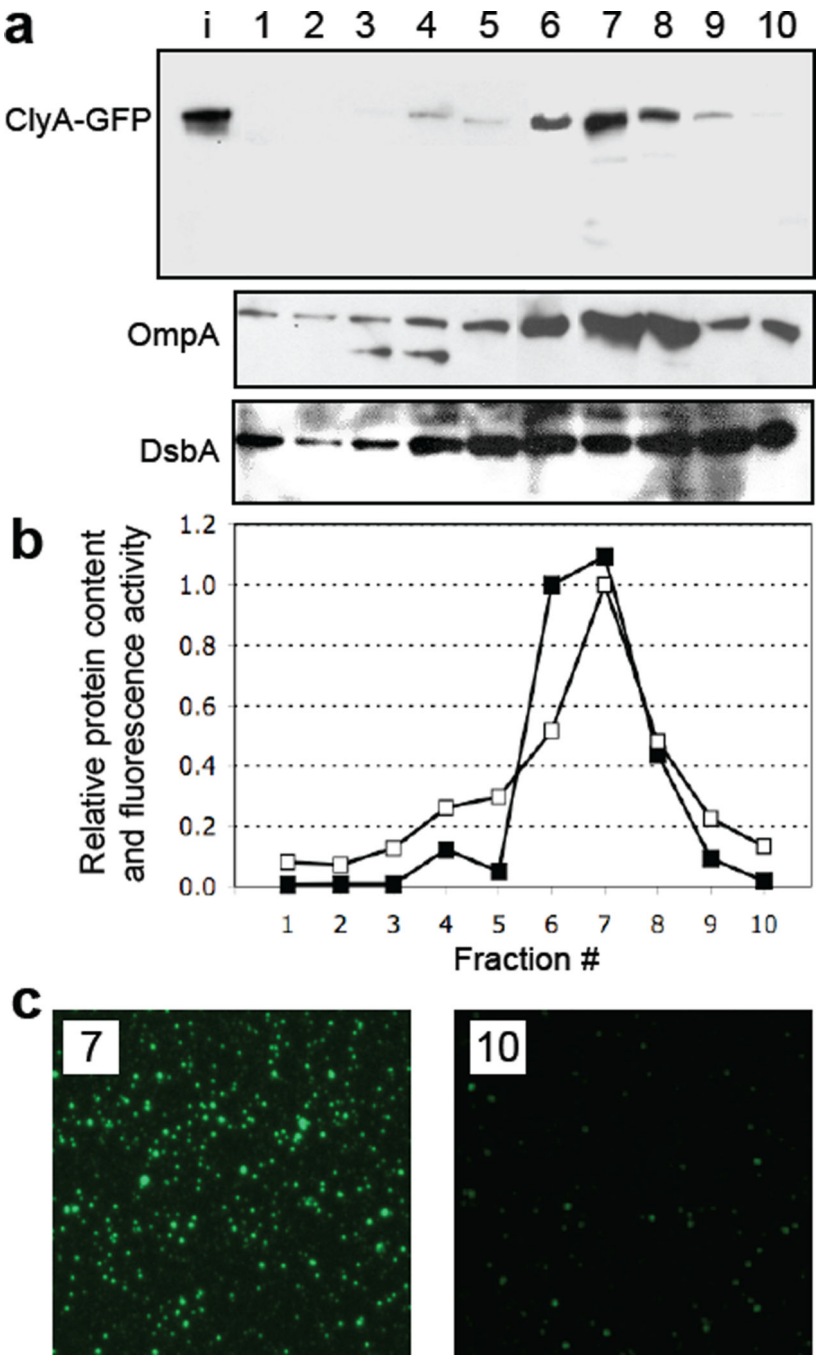

Figure 2.

Density gradient fractionation of vesicles. (a) Electrophoretic analysis of the density gradient fractions from top (lane 1, lowest density) to bottom (lane 10, highest density) from JC8031 cells expressing ClyA-GFP. The bands corresponding to ClyA-GFP (top), OmpA (middle) and DsbA (bottom) were obtained with anti-GFP, anti-OmpA and anti-DsbA serum, respectively. Lane i represents input vesicles from the purified cell-free supernatant. (b) Quantification of the ClyA-GFP levels (filled squared) in each fraction as determined by densitometry using ImageJ software. Band intensity values were normalized to the

maximum intensity corresponding to the ClyA-GFP measured in fraction 7. Also plotted is the GFP activity (open squares) measured in each fraction and normalized to the maximum activity, which also corresponded to fraction 7. (c) Fluorescence microscopy of vesicles that migrated in gradient fractions 7 and 10.

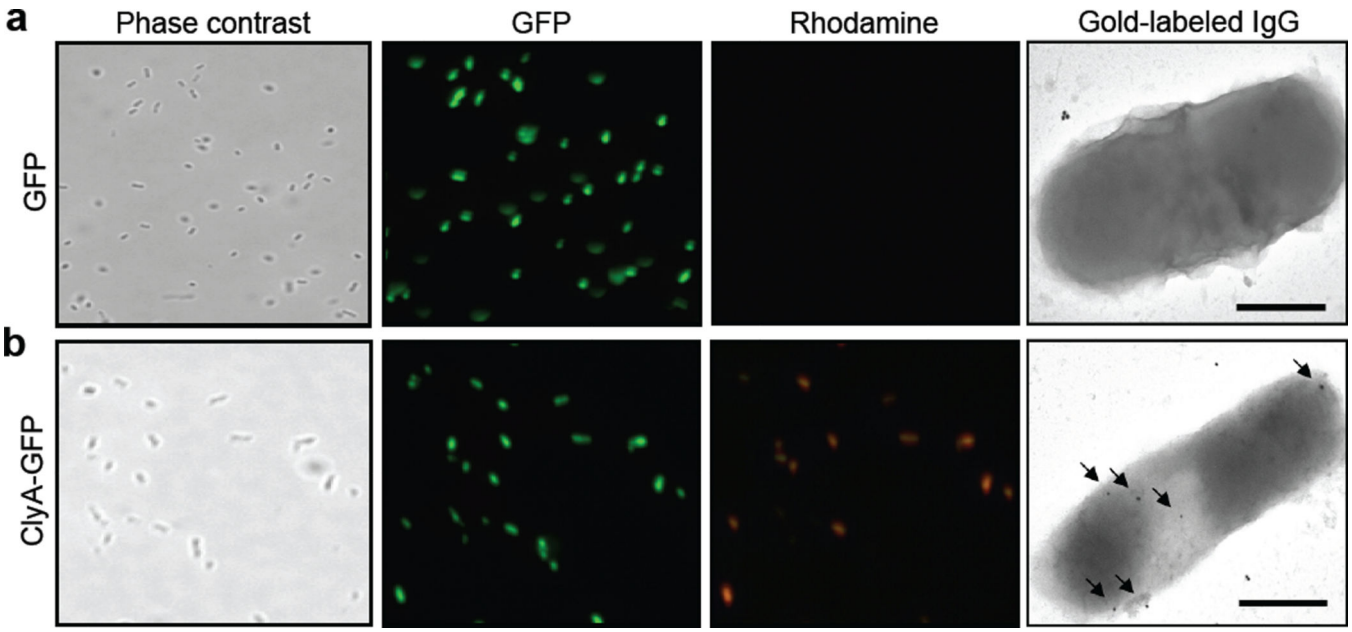

Figure 3.

Microscopic analysis of ClyA expression. JC8031 cells grown at 37°C in LB were induced to express (a) GFP and (b) ClyA-GFP. For immunofluorescence microscopy, cells were treated with mouse monoclonal anti-GFP and subsequently with rhodamine-conjugated anti-mouse IgG. Panels show phase contrast microscopy and fluorescence microscopy using green and red emission filters as indicated. For immunoelectron microscopy, cells were treated with mouse monoclonal anti-GFP and subsequently with gold-conjugated anti-mouse IgG. Arrows indicate the 25 nm gold particles. The bars are equal to 500 nm.

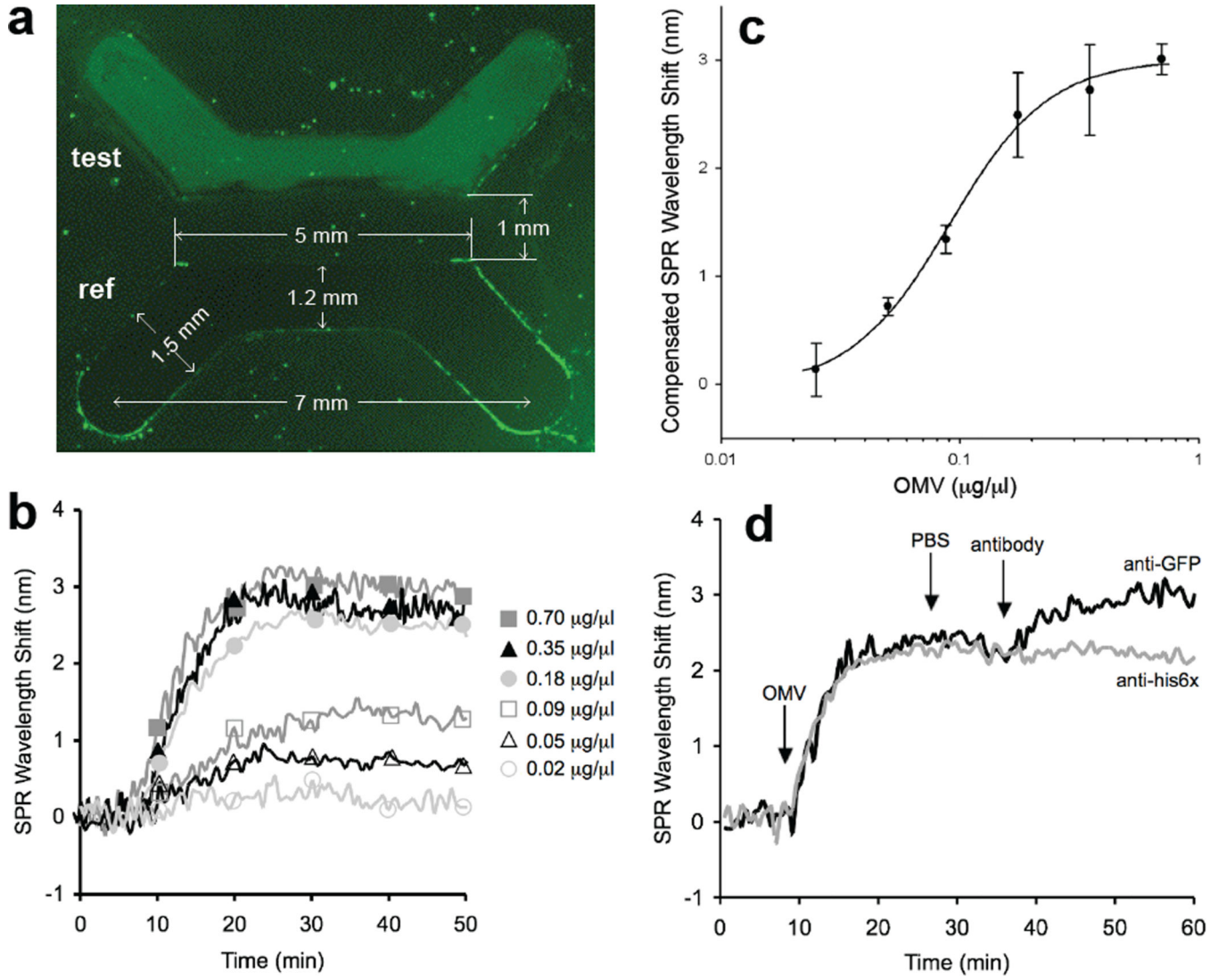

Figure 4.

Detection of vesicles and vesicle-associated antigens via immuno-SPR. (a) Fluorescence microscopy analysis of the binding of fluorescent s-MVs (at a concentration of 0.35 μg/μl) to anti-*E. coli* antibody in the test channel and to the BSA-treated surface in the reference channel following 20 min of s-MV binding and 20 min PBS rinse. The measurements indicated represent the size of the PDMS master. (b) Overlaid SPR sensorgrams showing concentration-dependent binding of OMVs to immobilized anti-*E. coli* antibodies. For each binding experiment, 200 μl of OMV-containing samples (diluted to the concentrations indicated) was introduced to the test or reference channel for 20 min, followed by a 20 min PBS rinse. The SPR signal was recorded as wavelength shift (nm) versus time and plotted as a “sensorgram”. All binding experiments were performed at 25°C ± 1°C with a flowrate of 10 μl/min. Each vesicle sample was assayed in triplicate and the standard error was determined to be less than 5%. (c) Vesicle standard curve generated using the SPR immunosensor. The steady-state SPR signal change was calculated by subtracting the average SPR signal during the PBS wash step following OMV binding from the average

SPR signal collected during the initial PBS wash step prior to OMV addition. The equation $y = 0.92\ln(x) + 3.63$ with an R^2 value of 0.95 describes the fit of a straight line through the logarithm of the data and was determined using SigmaPlot. The results are the average of the values calculated for the SPR signal change from three independent binding measurements with error bars showing ± standard error. It is noteworthy that the lower detection limit for this system was determined to be 0.01 μg/μl (10% of the compensated SPR wavelength shift in the standard curve) and that for vesicle concentrations ≥0.18 μg/μl, SPR wavelength shifts >2.5 nm were recorded, which is ~10× greater than the baseline signal. (d) Representative sensorgrams for antibody binding to s-MV surface-displayed GFP in test and reference channels. Channels were prepared identically so that fluorescent s-MVs were captured in both channels. The change in SPR signal over time was measured following addition of 1 μg/μl anti-GFP (black line) or 1 μg/μl anti-his6× (gray line) monoclonal antibody to surface-captured s-MVs. Antibody binding proceeded for 20 min followed by a 10 min PBS rinse. Each antibody was assayed in triplicate and the standard error was determined to be less than 5%.

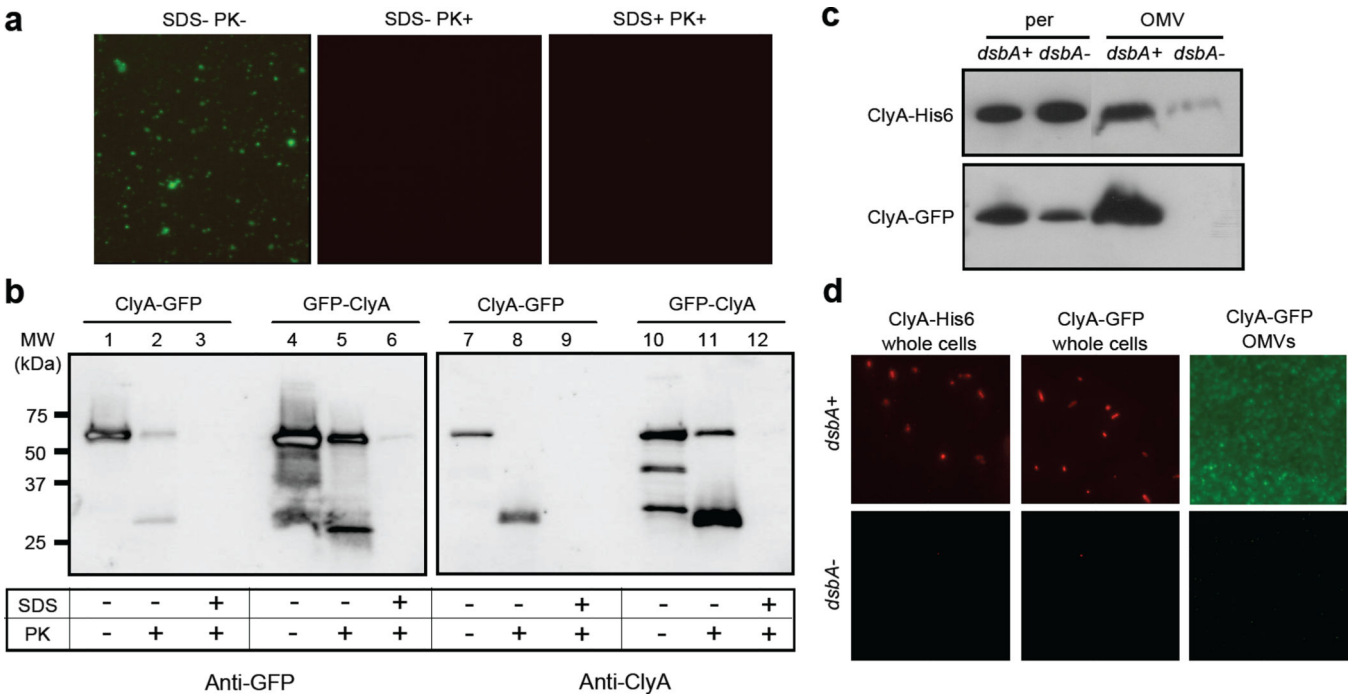

Figure 5.

Biochemical and genetic analysis of ClyA localization. Proteinase K susceptibility of OMV-tethered GFP as determined by: (a) fluorescence microscopy of vesicles generated from JC8031 cells expressing ClyA-GFP treated with Proteinase K and SDS as indicated; and (b) Western blot of vesicles generated from JC8031 cells expressing ClyA-GFP or GFP-ClyA. Blots were probed with mouse anti-GFP (left panels) or anti-ClyA serum (right panels). Molecular weight (MW) ladder is marked at left. An equivalent number of vesicles was used in all cases. (c) Western blot analysis of periplasmic and OMV fractions from JC8031 (*dsbA*+) and JC8031 *dsbA*::Kan cells (*dsbA*-) expressing either ClyA-GFP or ClyA-His6 as indicated. (d) Immunofluorescence (left and center panels) of wt JC8031 (*dsbA*+, top) and JC8031 *dsbA*::Kan cells (*dsbA*-, bottom) expressing pClyA-GFP or pClyA-His6 as indicated and fluorescence (right panel) of vesicles derived from the same cells as indicated. For immunofluorescence, cells were treated with either mouse monoclonal anti-GFP or anti-polyhistidine antibodies and subsequently with rhodamine-conjugated anti-mouse IgG.

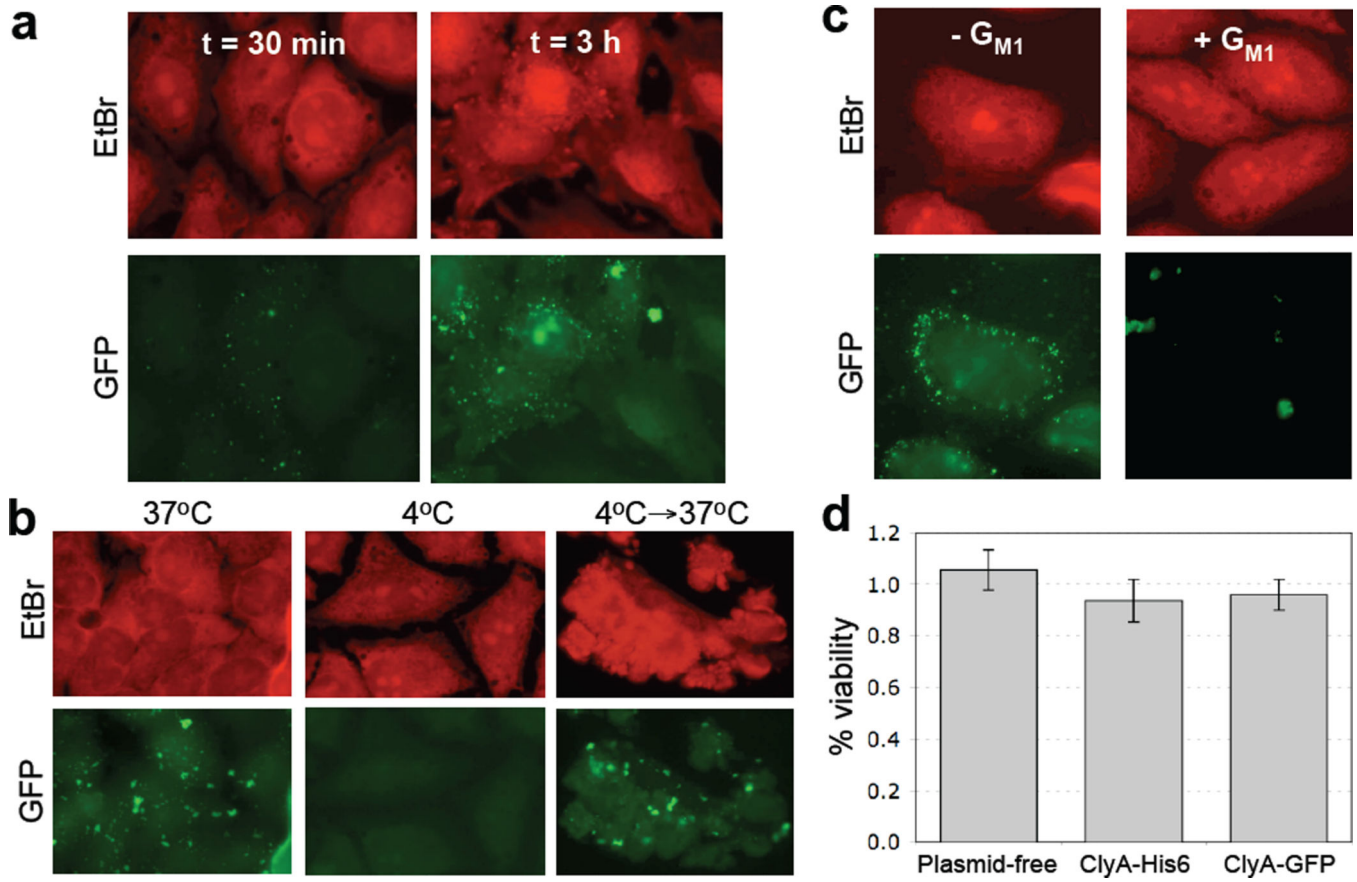

Figure 6.

Interaction of ClyA-GFP vesicles with HeLa cells. (a) OMVs containing ClyA-GFP were incubated with HeLa cells at 37°C for 30 min or 3 h as indicated. Fixed cells were stained with 0.5 mg/mL ethidium bromide (EtBr, upper panels) and visualized by fluorescence microscopy. (b) Temperature dependence of OMV-HeLa cell interactions was examined by incubation of HeLa cells with GFP-ClyA OMVs at the temperatures indicated. An equivalent number of OMVs (~150 μg) was used in all cases. (c) Untreated (− G_{M1}) or pretreated (+ G_{M1}) OMVs from JC8031 cells expressing ClyA-GFP were incubated with HeLa cells at 37°C for 3 h. Fixed cells were stained with 0.5 mg/mL ethidium bromide (EtBr, upper panels) and visualized by fluorescence microscopy. An equivalent number of OMVs (~150 μg) was used in all cases. (d) Cytotoxicity of vesicles as measured using the MTS assay with HeLa cell cultures. % viability is reported as the viability of vesicle-treated HeLa cells normalized to the viability following treatment with PBS. HeLa cells were treated with vesicle solutions derived from plasmid-free JC8031 cells and JC8031 cells expressing ClyA-His6, ClyA-GFP (dark gray). An equivalent number of OMVs (~150 μg) was used in all cases. Each sample was assayed in triplicate with error bars showing ± standard error.

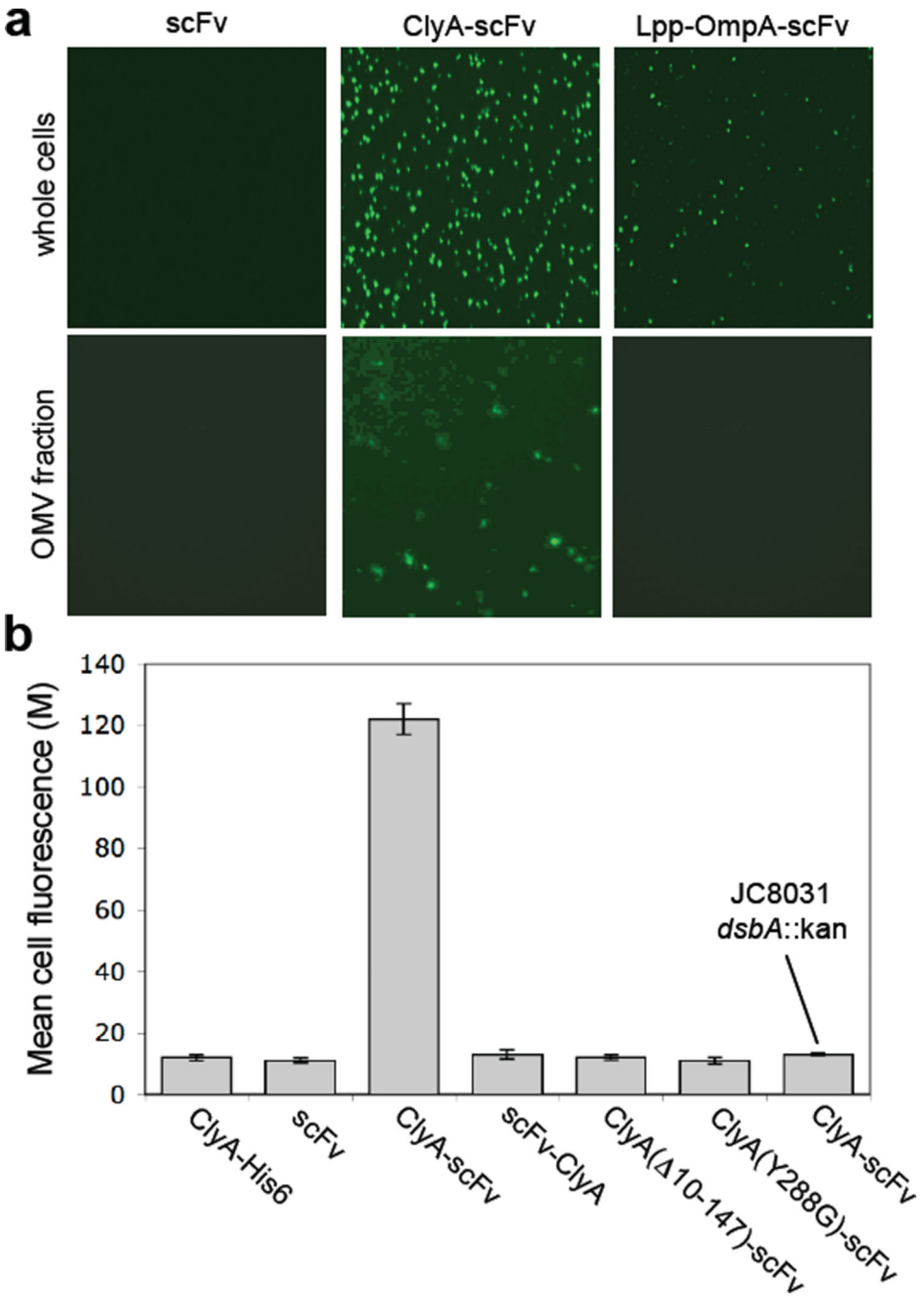

Figure 7.

Creation of immuno-MVs via ClyA-scFv chimeras. (a) Fluorescence microscopy of whole cells and vesicles generated from JC8031 cells expressing scFv.Dig, ClyA-scFv.Dig or Lpp-OmpA-scFv.Dig as indicated. For these studies, cells were grown and induced at room temperature followed by fluorescent labeling of cells or their derived vesicles with 1 μM Dig-BODIPY for 1 h at room temperature. (b) Genetic analysis of scFv.Dig localization was performed using flow cytometric analysis of strains and plasmids as indicated. Cells were grown and induced at room temperature followed by labeling with 1 μM Dig-BODIPY for 1

h at room temperature. Fluorescence is reported as the mean fluorescence for each cell population and was assayed in triplicate with error bars showing ± standard error.

Table 1

ClyA-mediated display of enzymatically active proteins

Construct	Cell surface activity	OMV activity
β-*lactamase* (*Bla*)	[ΔA486/min]	[ΔA486/min]
pBAD18-Kan	0.03	0.02
pΔss-Bla	0.47	0.98
pClyA-Bla	8.53	7.05
pBla-ClyA	1.43	1.65
Organophosphorus hydrolase (*OPH*)	[U*1000/OD_{600}]	[U*1000/g total protein]
pBAD24	0.09	0.04
pOPH	0.36	1.63
pClyA-OPH	11.62	81.63
pOPH-ClyA	0.22	8.19
β-*galactosidase* (*LacZ*)	[ΔA420/min]	[ΔA420/min]
pBAD24	0.02	0.02
pLacZ	0.02 (7.21)†	0.03
pClyA-LacZ	0.04 (8.33)†	0.03

†Values in parentheses represent activity in the cytoplasmic fraction.

All values represent the average of 3 replicate experiments where the standard error was <5%.

Table 2

Bacterial strains and plasmids used in this study

Bacterial strain or plasmid	Genotype/Description	Source
1292	*supE hsdS met gal lacY tonA*	[32]
JC8031	1292 Δ*tolRA*	[32]
BW25113	*lacI*^{q} *rrnB*$_{T14}$ Δ*lacZ*$_{WJ16}$*hsdR514* Δ*araBAD*$_{AH33}$ Δ*rhaBAD*$_{LD78}$	[64]
BW25113 *nlpI*::Kan	BW25113 *nlpI*::Kan created via the method of Datsenko and Wanner	[65]
DHB4	MC1000 *phoR* Δ (*phoA*) *PvuII* Δ (*malF*)*3* F′[*lacI*^{q}*ZYA pro*]	Laboratory stock
DHA	DHB4 *dsbA*::Kan	[66]
JCA	JC8031 *dsbA*::Kan	This study
pBAD18-Cm	*araBAD* promoter; pBR322 *ori* Cm^{r}	[67]
pBAD18-Kan	*araBAD* promoter; pBR322 *ori* Cm^{r}	[67]
pBAD24	*araBAD* promoter; pBR322 *ori* Amp^{r}	[67]
pClyA-His6	*E. coli clyA* carrying a C-terminal 6× polyhistidine tag cloned in pBAD18-Cm	This study
pGFP	*gfp-mut2* gene cloned in pBAD18-Cm	This study
pClyA-GFP	*clyA* gene fused to 5’ end of *gfp-mut2* in pBAD18-Cm	This study
pGFP-ClyA	*clyA* gene fused to 3’ end of *gfp-mut2* in pBAD18-Cm	This study
pΔss-Bla	Mature region of *bla* gene cloned in pBAD18-Kan	
pClyA-Bla	*clyA* gene fused to 5’ end of *bla* in pBAD18-Kan	This study
pBla-ClyA	*clyA* gene fused to 3’ end of *bla* in pBAD18-Kan	This study
pKEG01	*Flavobacterium* sp. *opd* gene in pET78UF	[68]
pOPH	*opd* gene cloned in pBAD24	This study
pClyA-OPH	*clyA* gene fused to 5’ end of *opd* in pBAD24	This study
pOPH-ClyA	*clyA* gene fused to 3’ end of *opd* in pBAD24	This study
pLacZ	*lacZ* gene cloned in pBAD24	This study
pClyA-LacZ	*clyA* gene fused to 5’ end of *lacZ* in pBAD24	This study
pB18D	anti-digoxin scFv fused to the 3’ end of *lpp-ompA* cloned in pBAD18	[58]
pB24D	anti-digoxin scFv fused to the 3’ end of *lpp-ompA* cloned in pBAD24	This study
pscFv.Dig	anti-digoxin scFv cloned in pBAD24	This study
pClyA-scFv.Dig	*clyA* gene fused to 5’ end of anti-digoxin scFv in pBAD24	This study
pscFv.Dig-ClyA	*clyA* gene fused to 3’ end of anti-digoxin scFv in pBAD24	This study
pClyA(Δ293–303)-scFv.Dig	*clyA* with 10 C-terminal residues removed	This study

Bacterial strain or plasmid	Genotype/Description	Source
pClyA(Δ156–303)-scFv.Dig	*clyA* with 147 C-terminal residues removed	This study
pClyA(Y288G)-scFv.Dig	*clyA* with Tyr288 residue mutated to Gly	This study